

JEZERO WATERSHED MAPPING OF OLIVINE-CARBONATE LITHOLOGY. A. J. Brown¹, T.A. Goudge², C.E. Viviano³ and F.P. Seelos³. ¹Plancius Research, Severna Park, MD (adrian.j.brown@nasa.gov) ²Jackson School of Geosciences, University of Texas, TX, 78712, ³Johns Hopkins Applied Physics Laboratory, MD, 20723

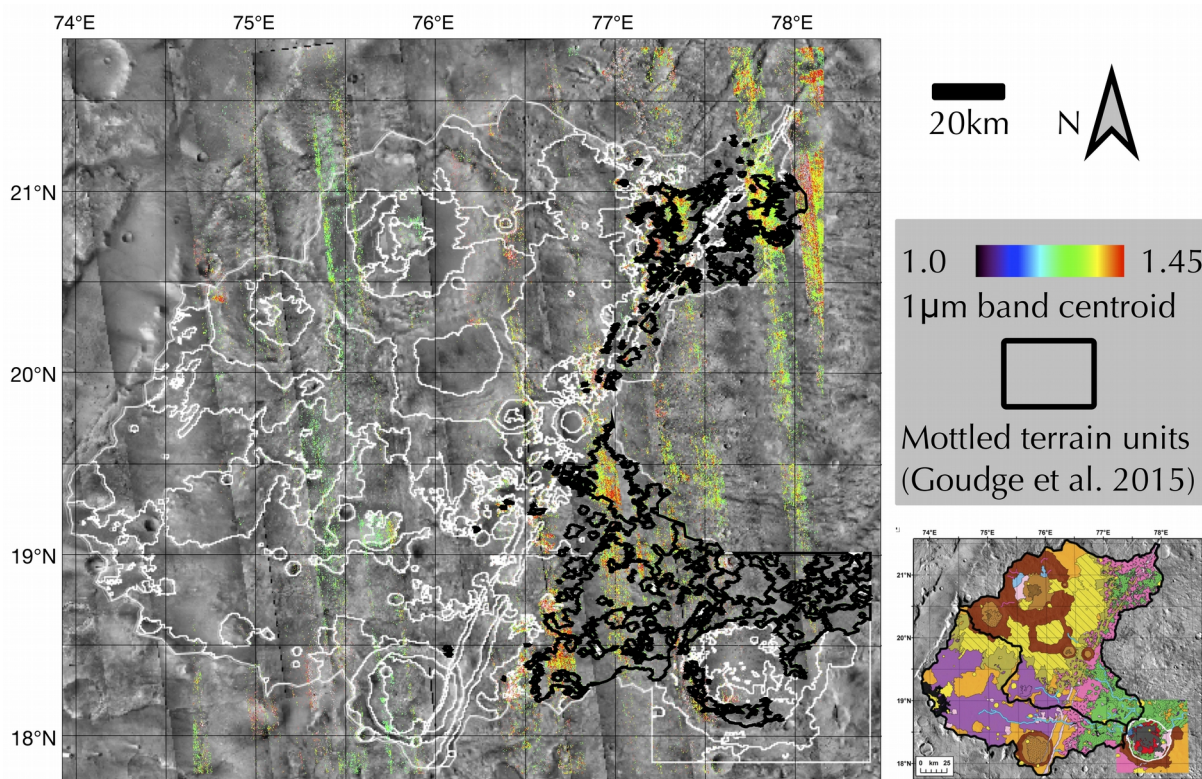


Fig. 1 – Olivine mineralogy of Jezero crater and watershed as mapped by an Asymmetric Gaussian technique on CRISM mapping images. Thin lines show the boundaries of major geomorphic units mapped by Goudge et al. [4], in bottom right inset.

Introduction: The Jezero Crater and its well exposed delta has been recently selected as the landing site for the Mars 2020 Rover [1]. Along with a number of other sites in the Nili Fossae region, Jezero is host to relatively large exposures of carbonate [2-3]. Using data from the CRISM instrument, we have mapped olivine and carbonate signatures present in Jezero Crater and its surrounding watershed. Here we show that by using the variations in the olivine 1 μm band we can map the olivine-carbonate unit throughout the watershed (Fig. 1).

Jezero Crater: Amongst the sites of interest in the Nili Fossae region is the paleolake basin contained within the ~45 km diameter Jezero impact crater. The Jezero crater paleolake is classified as hydrologically open, and is fed by two inlet valleys to the north and west, and drained by an outlet valley to the east [5]. Buffered crater counts of the fluvial valleys associated with the Jezero paleolake indicate that this system ceased activity by approximately the Noachian-Hesperian boundary, similar to the timing of other large valley network systems on Mars [5-7].

Methods: We used CRISM tiled multispectral datasets [8] and an iterative Asymmetric Gaussian approach [9] to track variations in band center and shape and produce an olivine-discriminating map of the Jezero crater watershed. We applied a threshold to the four parameters of the fit (centroid, asymmetry, width and amplitude) to eliminate noisy and non-olivine bearing pixels.

Results: In Fig. 1 we present a comparison of the Asymmetric Gaussian map with the existing geomorphic map produced by Goudge et al. [4]. Outlined in black is the “mottled unit” that [4] associated with the olivine-carbonate lithology. Shown in rainbow colours is the centroid position of the 1 μm band for those pixels which pass the threshold test, which we suggest is associated with the olivine-carbonate lithology. There are areas of good agreement to the west and north west of Jezero crater, however there are also areas that were outside of the map in [4] showing up along the eastern edge of our image. We are using our CRISM observations to improve our understanding of the map of [4].

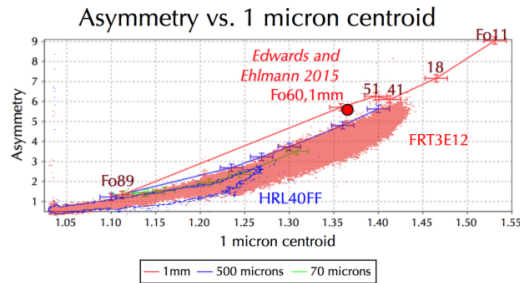


Fig. 2 - “Shkuratov plot” showing dependence of olivine centroid and asymmetry parameter on composition and grain size. The points from **FRT3E12** (red) and **HRL40FF** (outlined blue) are plotted to show the CRISM results.

Discussion: Fig. 2 shows a “Shkuratov plot” inspired by Figure 11 of [10]. It plots the relationship between the asymmetry and the 1 μm centroid position for the olivine 1 μm band, for different Fo # of olivine spectra from [11]. The coloured lines correspond to grain sizes ranging from 70 microns to 1mm. Fo# points are labeled on the red line only, they are transferrable to the blue and green lines. This shows the effect of variable grain size and composition on the olivine 1 μm band. We have also plotted the results of our Asymmetric Gaussian fit for CRISM FRT 3E12 (red shading) and HRL40FF (blue outline) from the Jezero crater watershed.

Edwards and Ehlmann [12] carried out a Hapke fit to a CRISM spectrum in Nili Fossae (FRT C968), north of Jezero, in the olivine-carbonate lithology. They reported an olivine of 1mm grain size and Fo60 was required to fit the olivine 1 μ m band adequately. We plot their result in Fig. 2, and note two things:

1.) The Edwards and Ehlmann spot measurement is reasonable for the location from which it was taken (it corresponds to an extreme upper of the red shading range of FRT3E12), however is not indicative of the full range of olivine composition. The points from 3E12 (red shaded in Fig. 2) have a considerable tail that extends to the right of the [13] Fo60 estimate. This corresponds to a centroid of $\sim 1.43\mu\text{m}$, which intersects the red 1mm line just to the right of Fo41. Assuming a grain size of 1mm allows us to place a lower bound of Fo40 on the composition of the olivine in FRT3E12, where it is best exposed.

2.) Fig. 2 gives us a way to place an upper and lower limit on the grain size of the olivine in FRT3E12. We do this in two different ways. A maximal value of 1mm brackets the top values of the red shaded area, and a lower limit of 500 microns is required to fit the range of asymmetry/centroid observations. Lower grain sizes (e.g. the green 70 micron curve) cannot explain our observations in FRT 3E12.

Fig. 3 lists olivine composition for Martian samples analysed to date (in situ, remotely and in the meteorite collection), showing that even at the finest

scale of EMP analysis, olivine shows a range of compositions [13]. We also note that martian olivine is more Fe-rich than their terrestrial counterparts, having formed in a Fo77 mantle, rather than Fo89 [14].

Take away messages: 1. We have used CRISM tiled mapping datasets to map variations in the shape and centroid of the olivine 1 μm band in the Jezero crater and watershed (Fig. 1) and shown that this largely corresponds to previous mapping of “mottled terrain” associated with the Nili Fossae olivine-carbonate lithology [4].

2. We have used the variability of the olivine 1 μm band in the Jezero watershed to place bounds on the grain size and Fo# of the olivine-carbonate lithology (Fig. 2). Our observations show that where the olivine is best exposed (e.g. FRT 3E12) the olivine grain size must be at least 500 microns, and at most 1mm. Assuming the grain size is 1mm allows us place a lower bound on the composition of the exposed olivine-carbonate lithology as Fo40 (Fig. 3).

Acknowledgements: Work supported by NAI grant #NNX15BB01A/MDAP grant #NNX16AJ48G.

References: [1] Williford K. et al (2018) Mars2020 A Progress Report “*Mars: Habitability to Life*” eds. Cabrol, N. and Grin, E. [2] Ehlmann B. et al (2008) *Science* **322** [1828](#) [3] Niles, P. et al (2012) *SSR* **174** [301-328](#) Wray, J. et al (2016) *JGR* **121** [652-677](#) [4] Goudge, T. et al. (2015) *JGR* **120** [775-808](#) [5] Fassett C. and Head J. (2005) *GRL* **32** [L14201](#) [6] Fassett, C. and Head, J. (2008) *Icarus* **198** [37-56](#) [7] Goudge, T. et al. (2017) *EPSL* **458** [357-365](#) [8] Seelos, F. *this meeting* [9] Brown, A. et al (2010) *EPSL* **297** [174-182](#) Brown, A. (2006) *TGARS* **44** [1601-8](#) [10] Shkuratov, Y. et al. (1999) *Icarus* **137** [235-246](#) [11] King, T. and Ridley, W. (1987) *JGR* **92** [11457](#) [12] Edwards, C. and Ehlmann, B. (2015) *Geology* **43** [863-6](#) [13] McSween, H. et al (2006) *JGR* **111** [E02S10](#) [14] Dreibus, G. and Wanke, H. (1985) *Meteoritics* **20** [367-381](#)

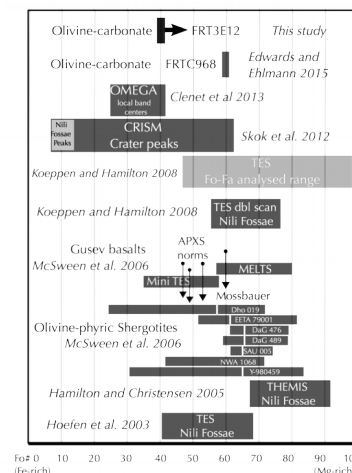


Fig. 3 – Previous composition results for Martian olivine bearing rocks, after [9]. Results from this study are shown at the top.